Int J Thermophys (2010) 31:1195–1211
DOI 10.1007/s10765-010-0826-5

Temperature-Dependent Thermal Conductivity of High Strength Lightweight Raw Perlite Aggregate Concrete

Ahmet Tandiroglu

Received: 29 October 2009 / Accepted: 13 September 2010 / Published online: 28 September 2010

Abstract Twenty-four types of high strength lightweight concrete have been designed with raw perlite aggregate (PA) from the Erzincan Mollaköy region as new low-temperature insulation material. The effects of the water/cement ratio, the amount of raw PA, and the temperature on high strength lightweight raw perlite aggregate concrete (HSLWPAC) have been investigated. Three empirical equations were derived to correlate the thermal conductivity of HSLWPAC as a function of PA percentage and temperature depending on the water/cement ratio. Experimentally observed thermal conductivities of concrete samples were predicted 92 % of the time for each set of concrete matrices within 97 % accuracy and over the range from $1.457\,\mathrm{W \cdot m^{-1} \cdot K^{-1}}$ to $1.777\,\mathrm{W \cdot m^{-1} \cdot K^{-1}}$. The experimental investigation revealed that the usage of raw PA from the Erzincan Mollaköy region in concrete production reduces the concrete unit mass, increases the concrete strength, and furthermore, the thermal conductivity of the concrete has been improved. The proposed empirical correlations of thermal conductivity were considered to be applicable within the range of temperatures $203.15\,\mathrm{K} \leq T \leq 303.15\,\mathrm{K}$ in the form of $\lambda = a(PAP^{b}) + c(T^{d})$.

Keywords Heat transfer · High strength lightweight concrete · Thermal conductivity

A. Tandiroglu
Department of Mechanical Engineering, Faculty of Engineering,
Erzincan University, 24100 Erzincan, Turkey

A. Tandiroglu (✉)
Erzincan Üniversitesi, Mühendislik Fakültesi, Makine Mühendisliği Bölümü, 24109 Erzincan, Turkey
e-mail: atandiroglu@erzincan.edu.tr

List of Symbols

Q	Power per unit length of the heating line source, $W \cdot m^{-1}$
PAP	Perlite aggregate percentage by mass, %
r	Radial position, m
t	Time, s
T	Temperature, K
w/c	Water cement ratio, %

Greek Symbols

α	Thermal diffusivity, $m^2 \cdot s^{-1}$
λ	Thermal conductivity, $W \cdot m^{-1} \cdot K^{-1}$
γ	Euler's constant (0.5772…)

1 Introduction

Lightweight concrete is generally used to reduce the dead weight of a structure as well as to reduce the risk of earthquake damage to a structure because the earthquake forces that will influence the civil engineering structures and buildings are proportional to the mass of those structures and buildings. Thus, a reduction in mass of the structure or building is of utmost importance to reduce the risk due to earthquake acceleration [1]. It is a well-known fact that the thermal conductivity of high strength lightweight raw perlite aggregate concrete (HSLWPAC) ingredients (cement paste and aggregates) are different from each other. Therefore, temperature changes in HSLWPAC cause differential volume changes in the ingredients, and these changes can result in cracking and lower durability [2–4]. Structural lightweight concretes (LWCs) produced by pumice and concretes with normal-weight aggregate (NWC) were investigated [5]. Concrete of low thermal conductivity is useful for the thermal insulation of buildings [6]. The thermal conductivity of concrete increases with increasing cement content [7] and thermal conductivity of the aggregate [8,9]. Bouguerra et al. [10] reported that the thermal conductivity of LWC changes considerably with porosity [11].

There are some investigations and literature surveys on the thermal conductivity and compressive strength of low strength concrete incorporated with mineral admixtures [12,13]. The thermal conductivity of limestone from Gaziantep in Turkey has been investigated [14]. The limestone samples were collected from different parts of the city representing Gaziantep and Fırat formations which are clay and chalky limestone. The thermal conductivity of the samples was measured for saturated, partially saturated, and dried conditions. Water absorption, dry unit mass, and apparent porosity of the samples were also measured to correlate with thermal conductivity. Measurements showed that the thermal conductivity increased with an increase in the water content of samples. The thermal conductivity of the samples decreased when the porosity increased. Relationships between the thermal conductivity and both dry unit mass and porosity were developed. There was a very good exponential relationship between the thermal conductivity and saturation degrees of the sample, the porosity, and an increase in the density. The moisture content increased the thermal conductivity by up to 113 %. A review of earlier studies reveals that the mineralogical character of the aggregate can greatly influence the thermal conductivity of concrete. Aggregates with a lower thermal conductivity produce concrete with a lower thermal conductivity [15]. Thus, the aggregate type can result in a factor of two increase in the thermal conductivity of concrete, and this depends not only on the aggregate composition but also on its degree of crystallization.

The thermal conductivity of concrete with an aggregate has been presented in the literature [16]. Uysal et al. [11] reported that the density of concrete increased with an increase in the cement dosage (keeping the slump constant at (3 ± 1) cm). When the cement dosage increased from 200 $kg{\cdot}m^{-3}$ to 250 $kg{\cdot}m^{-3}$, 350 $kg{\cdot}m^{-3}$, 400 $kg{\cdot}m^{-3}$, and 500 $kg \cdot m^3$, the thermal conductivity increased by 3.4 %, 5.2 %, 9.4 %, and 25.6 %, respectively. The perlite aggregate (PA) decreased the density and thermal conductivity of concretes up to 40 % and 46 %, respectively. The effects of the different slumps on the density and thermal conductivity fluctuated. Topcu [17] and Al-Khaiat and Haque [18] reported that structural lightweight concrete has its obvious advantages of higher strength/mass ratio, better tensile strain capacity, lower coefficient of thermal expansion, and superior heat and sound insulation characteristics due to air voids of the lightweight aggregate. Kılıç et al. [19] presented a part of the results of an ongoing laboratory study carried out to design a structural lightweight high strength concrete (SLWHSC) made with and without mineral admixtures. In the mixtures, basaltic-pumice (scoria) was used as a lightweight aggregate. Based on the results of experimental work, the scoria lightweight aggregate can be used in the production of SLWC. The use of a nonstandard fly ash, which will reduce the cost and environmental pollution, is possible for both fly ash SLWC and ternary mixtures. It is possible to produce a lightweight concrete with a 40 MPa cylinder compressive strength by the use of silica fume. The use of mineral additives in structural lightweight concrete can reduce the dead weight further and increase the strength. In summary, the lightweight scoria aggregate can be utilized in its locality to reduce the risk of earthquake acceleration by using it in the production of SLWC and SLWHSC.

Recently, the production of high strength lightweight concrete using Erzincan Mollaköy raw PA has been investigated [20] to a limited extent. It is concluded that high strength concretes with densities between 1830 $kg \cdot m^{-3}$ and 1915 $kg \cdot m^{-3}$ can be made with or without the use of mineral admixtures, but the use of a super plasticizer is mandatory. The highest compressive cubical strength achieved was 110 MPa at 90 days for cement content of 660 $kg \cdot m^{-3}$. The results of analysis indicate that the water/cement ratio is an important parameter that influences the mechanical and physical properties of concrete. Also, the cement content and cement type effect these properties. The steel fiber did not effect the compressive strength, but increases the tensile strength about 70 % along with the brittleness of concrete. The elastic modulus of concrete varies between 17.25 GPa and 25.5 GPa. Pozzolanic properties of perlite and perlite's usability in cement production have been investigated [21]. For this purpose, perlites from two different sources—Izmir and Erzincan—are used as replacements of portland cement clinker with two different percentages: 20 % and 30 % by mass of total cement. Then for each different composition, materials are ground with some gypsum in order to obtain grinding curves for the resultant cements. After obtaining the grinding curves, a total of 22 cements with two different finenesses are produced by intergrinding and separately grinding the materials for each composition. The obtained cements are used in paste and mortar production so that normal consistencies, setting times, autoclave expansions, and compression strengths are determined.

The usage of raw PA in high strength lightweight concrete production has many properties that makes them suitable for thermal insulation due to a low thermal conductivity. PA is used to provide thermal insulation especially ideal for cryogenic insulation and insulating panels, boards, and tiles. The raw PA content, sieve sizes of raw PA, cement content, and water/cement ratio play important roles in determining the thermal conductivity of high strength lightweight concrete.

To date, there has not been an intensive study to analyze and correlate the dependence of the thermal conductivity of high strength lightweight concrete production by using raw perlite aggregate from the Erzincan Mollaköy region in Turkey. The main objective of the present work is to derive empirical equations to correlate the thermal conductivity depending on the water/cement ratio (w/c), the raw perlite amount by mass (*PAP*), and the temperature (T). The proposed thermal conductivity correlations are considered to be applicable within the range of the temperatures $203.15\,\mathrm{K} \leq T \leq 303.15\,\mathrm{K}$ for the case of HSLWPAC from the Erzincan Mollaköy region in Turkey.

2 Materials

Well-graded different grain sizes of raw perlite supplied from the Erzincan Mollaköy region were used as an aggregate to produce high strength lightweight concrete for low-temperature and cryogenic applications. Number 43 grade ordinary Portland cement, equivalent to Type I of ASTM Standard, conforming to I.S. 8119, was used for the production of the high strength lightweight concrete. The chemical composition of the raw PA which was used to produce high strength lightweight concrete was determined in accordance with ASTM C311 [22] and given [23] in Table 1.

The raw PA was separated according to size. It was sieved using standard sieves and separated into eight groups in grain sizes of (15 to 12.5) mm, (12.5 to 9.5) mm, (9.5 to 6.7) mm, (6.7 to 5.66) mm, (5.66 to 4.00) mm, (4 to 2.36) mm, (2.36 to 1.18) mm, and (1.18 to 0) mm. The physical properties of fixed grain-size fractions of the raw PA are given in Table 2.

Table 1 Chemical composition of raw perlite

Chemical composition	Mass%
SiO_2	70.96
Al_2O_3	13.40
Fe_2O_3	1.16
MgO	0.28
CaO	1.72
Na_2O_3	3.20
K_2O	4.65

Table 2 Physical properties of raw perlite aggregate

Properties	Raw perlite grain diameter (mm)							
	15–12.5	12.5–9.5	9.5–6.7	6.7–5.66	5.66–4.0	4–2.36	2.36–1.18	1.18–0
Perlite usage ($kg \cdot m^{-3}$)	150	150	150	150	150	150	150	150
Bulk density ($kg \cdot m^{-3}$)	1066	909	868	1771	1393	1436	873	888
Compressed density ($kg \cdot m^{-3}$)	1132	981	934	1959	1553	1627	1028	1073
Specific gravity ($g \cdot cm^{-3}$)	1.87	1.89	1.92	1.95	1.97	1.99	2.01	2.05
Water absorption (%)	7.04	6.46	5.87	4.40	2.64	1.99	1.94	1.91
Water absorption in 30 min (%)	3.32	3.13	2.73	2.15	1.76	1.62	1.45	1.35

Details of high strength lightweight concrete proportions are given in Table 3. In the mixing of high strength lightweight concrete production, five different cement contents and eight different diameters of raw PA were used for three different w/c ratios of 0.4, 0.5, and 0.65. A super plasticizer was used to improve the workability of the specimens. In all cases, the amount of total raw PA was constant, and the content of water and cement was adjusted in order to obtain mixtures with the target w/c ratios and similar consistency. Potable water was used for concrete production.

Cylindrical test specimens of 100 mm dia. × 200 mm height and cubical test specimens of $150 \times 150 \times 150\,mm^3$ were prepared as three samples for each concrete mixture. The total number of 270 concrete specimens were cast and stored in lime saturated water at (296.15 ± 1) K until compressive strength testing showed that the concrete hardened in accordance with the requirements of ASTM C192. After a curing period of 28 days, water absorption percentages were calculated for each concrete sample.

For each concrete mixture, three samples of $150 \times 100 \times 50\,mm^3$ prisms were cast for thermal-conductivity tests. The 45 concrete specimens were dried for 28 days in an oven at (383.15 ± 10) K and weighed at 24 h intervals until the loss in mass did not exceed 1 % in 24 h in accordance with ASTM C 332. The specimens' surfaces were smoothed with sandpaper before measuring their thermal conductivities. Compressive strength tests were also performed. There is common agreement that concrete with a compressive strength greater than 50 MPa after 28 days is generally regarded as high strength concrete. Compressive strength tests and dry bulk density tests were performed according to ASTM C39 and ASTM C567-91 specifications [24,25] and tabulated with concrete mixture designations in Table 3.

3 Experimental Technique and Measurements

3.1 Thermal-Conductivity Measurement Theory

The dynamic method known as the hot-wire method is based on an idealized "one-dimensional radial heat flow" model. In Fig. 1, a schematic representation of the radial heat flow model is shown. The hot-wire method is a transient dynamic technique based

Table 3 Details of high strength lightweight concrete mix proportions in m^3

Water cement ratio by mass (w/c)	Cement content $(kg \cdot m^{-3})$	Concrete designation	Strength of concrete (MPa) (ASTM C39)	Water absorption (%) (ASTM C567-91)		Dry bulk density $(kg \cdot m^{-3})$ (ASTM C567-91)	
				Water cured	Sprite cured	Water cured	Sprite cured
0.4	450	S4C450	63	6.90	7.20	1838	1816
	475	S4C475	67	6.70	7.00	1844	1824
	500	S4C500	70	6.50	6.80	1848	1831
	525	S4C525	71	5.60	5.90	1854	1844
	550	S4C550	73	5.20	5.50	1858	1853
	575	S4C575	75	4.90	5.20	1864	1856
	600	S4C600	76	4.60	4.90	1868	1858
	625	S4C625	78	4.50	4.95	1874	1867
	650	S4C650	80	4.40	4.75	1883	1875
0.5	450	S5C450	62	7.00	7.20	1800	1774
	500	S5C500	65	6.85	7.10	1808	1785
	525	S5C525	67	6.73	7.06	1814	1763
	550	S5C550	69	6.62	7.00	1818	1828
	575	S5C575	71	6.53	6.92	1831	1831
	600	S5C600	73	6.45	6.85	1842	1833
	625	S5C625	74	6.39	6.77	1846	1834
	650	S5C650	75	6.35	6.70	1849	1836
0.65	450	S65C450	60	7.75	8.15	1798	1792
	500	S65C500	63	7.40	7.65	1805	1800
	550	S65C550	67	7.20	7.45	1809	1804
	575	S65C575	69	6.87	7.33	1812	1807
	600	S65C600	70	6.50	7.20	1814	1811
	625	S65C625	72	6.47	7.00	1822	1817
	650	S65C650	73	6.40	6.80	1828	1819

on a linear heat source of infinite length and an infinitesimal diameter and on the measurement of the temperature rise at a defined distance from the linear heat source embedded in the test material as shown in Fig. 2. As a constant electric current flows through the wire, the thermal conductivity can be derived from the resulting temperature change over a known time interval.

The ideal mathematical model is based on the assumption that the hot wire is infinitely thin and a long-line continuous heat source. It produces a thermal pulse for a finite time with a constant heating power and generates isothermal conditions in an infinite homogeneous medium initially at equilibrium. The transient temperature, for a sufficiently long time from the start of the heat generation, can be expressed with good approximation by the form [26],

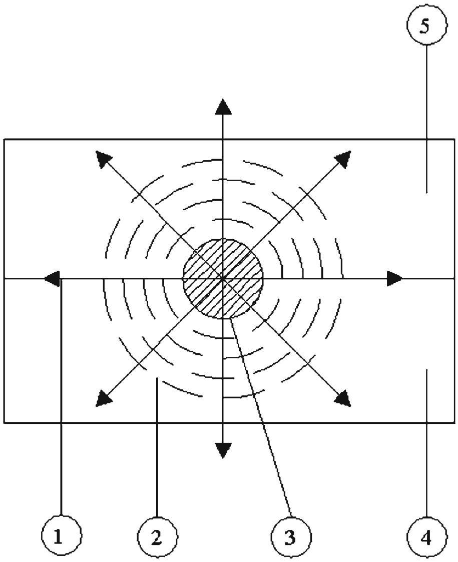

Fig. 1 Radial heat flow model. *1* Heat flow, *2* isothermal line, *3* hot wire, *4* and *5* sample

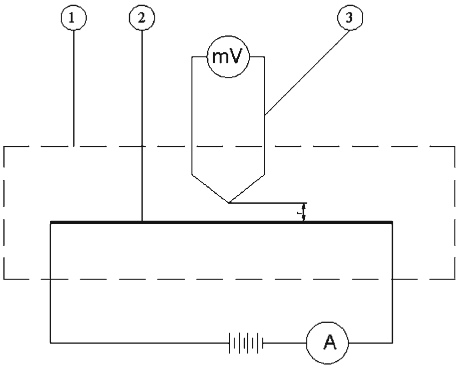

Fig. 2 Physical principle of hot-wire method. *1* Sample, *2* hot wire, *3* thermocouple

$$T(r,t) = \frac{Q}{4\pi\lambda}\left[\ln\left(\frac{4\alpha t}{r^2}\right) + \frac{r^2}{4\alpha t} - \frac{1}{4}\left(\frac{r^2}{4\alpha t}\right) - \cdots - \gamma\right] \tag{1}$$

where λ is the thermal conductivity $(\mathrm{W}\cdot\mathrm{m}^{-1}\cdot\mathrm{K}^{-1})$, Q is the power supply per unit length of the heating line source $(\mathrm{W}\cdot\mathrm{m}^{-1})$, α is the thermal diffusivity of the sample $(\mathrm{m}^2\cdot\mathrm{s}^{-1})$, r is the radial position where the temperature is measured, and $\gamma = 0.5772156$ is Euler's constant.

Since the term inside the parenthesis is negligible for sufficiently long times,

$$\left(\frac{r^2}{4\alpha t}\right) \ll 1 \tag{2}$$

and the temperature can be expressed with good approximation by the simplified form,

$$T(r,t) = \frac{Q}{4\pi\lambda}\left[\ln\left(\frac{4\alpha t}{r^2}\right) - \gamma\right] \tag{3}$$

that can also be written as

$$T(r,t) = \frac{Q}{4\pi\lambda}\left[\ln t + \ln\left(\frac{4\alpha t}{r^2}\right) - \gamma\right] \tag{4}$$

If the temperatures are measured at times t_1 and t_2 within the validity range of Eq. 2, then for a time interval $\Delta T = t_2 - t_1$, the rise in temperature at a point in the medium is given by

$$\Delta T = T_{t_2} - T_{t_1} = \frac{Q}{4\pi\lambda}\ln\left(\frac{t_2}{t_1}\right) \tag{5}$$

Thus, rearranging Eq. 5 gives the thermal conductivity, λ, in the form,

$$\lambda = \frac{Q}{4\pi\left[T_{t_2} - T_{t_1}\right]}\ln\left(\frac{t_2}{t_1}\right) \tag{6}$$

3.2 Experimental Setup

A schematic diagram of the experimental setup is presented in Fig. 3. The experimental setup consists mainly of a temperature test chamber and data acquisition system. A commercially available Vötsch VT7011 type temperature test chamber was used to provide constant programmable temperatures from 203.15 K to 453.15 K.

A total of 72 concrete specimens of $150 \times 100 \times 50\,\text{mm}^3$ dimensions were tested by using a QTM-500 quick thermal-conductivity meter and an Ahlborn Almemo thermal-conductivity probe to determine and establish the relationship between the temperature and thermal conductivity of the specimens.

The test chamber is equipped with a programmable temperature controller unit to provide a constant isothermal test temperature environment. The thermal-conductivity

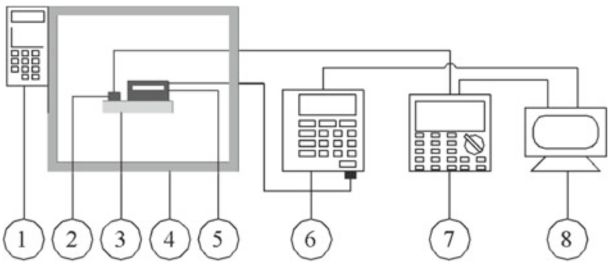

Fig. 3 Schematic diagram of experimental setup. *1* Temperature controller unit, *2* thermal-conductivity sensor, *3* concrete sample, *4* test chamber, *5* thermal-conductivity probe, *6* Thermal-conductivity meter, *7* data online acquisition system, *8* personal computer

meter and thermal-conductivity probe were connected to the inner part of the test chamber by drilling two holes on the inner part of the test chamber, so that measurement cables were passed through the test chamber. Hollow phenolic tubes are inserted into the holes, as a shield, and sealed to protect the cables from damage and heat leaks. The experiments were conducted for all concrete specimens after the surfaces of all samples were polished to achieve smooth surfaces in order to maintain proper contact between the thermal-conductivity sensor and probe to the specimen. The effect of thermal radiation for internal flow is ignored during the experiments due to the small temperature difference between the test chamber interior wall and the concrete samples. For each concrete sample, the thermal conductivity was measured three times, and the mean values were used in the analysis. It was observed that the maximum variation of thermal-conductivity values for the identical specimens did not exceed 1.5 %.

The thermal-conductivity probe of QTM-500 and thermal-conductivity sensor of type Almemo FTA3901 with special measurement range from 173.15 K to 673.15 K were installed on concrete specimens to perform fast and easy determination of thermal conductivities.

As is well known, QTM-500, a quick thermal-conductivity meter based on the ASTM C 1113-90 hot-wire method was used to measure the thermal conductivity in the following manner. The hot-wire test is a transient method and therefore overcomes the problem of moisture migration and subsequent decrease in thermal conductivity that would occur with a steady-state method. A constant electrical current is applied to a pure platinum wire placed between two bricks. The rate at which the wire heats is dependent upon how rapidly heat flows from the wire into the constant temperature mass of the sample. The rate of temperature increase of the platinum wire is accurately determined by measuring its increase in resistance in the same way a platinum resistance thermometer is used. A Fourier equation is used to calculate the k-value based on the rate of temperature increase of the hot wire and the power input [27]. Measurement range of QTM-500 is $0.0116\ \mathrm{W \cdot m^{-1} \cdot K^{-1}}$ to $6\ \mathrm{W \cdot m^{-1} \cdot K^{-1}}$. The measurement precision is ± 5 % of the reading value per reference plate. The reproducibility is ± 3 % of the reading value per reference plate. The temperature measurement range is 173.15 K to 1273.15 K (external bath or electric furnace for temperature). Measuring time is normally 100 s to 120 s. This method has wide applications [28–30] in determining the thermal conductivity of refractory materials where, instead of measuring the heat flow, the temperature variation with time at certain locations is measured. Being transient in nature, this method takes only a few minutes in contrast to other methods involving steady-state conditions.

The Almemo 5590-2 data online acquisition system is used with the heatable thermal-conductivity sensor FTA3901, which feeds a constant heat flow into the test material until a balance is established between input thermal energy and output thermal energy from the material. Thermal-conductivity sensors of type FTA3901 have ± 0.05 % full scale accuracy, and no sensor calibration settings are required because of common features of all Almemo sensors. The intelligent Almemo connectors are patented and have been especially designed for directly connecting more than 65 types of sensors such as temperature, rotating vane air flow meter, differential pressure, and peripheral equipment. Accurate measuring data can be read immediately without requiring instrument calibration settings.

Data for the thermal conductivity measuring probe and sensor were recorded and finally averaged over the elapsed time simultaneously until the system was allowed to approach a steady state.

4 Results and Discussion

Figure 4 shows the thermal conductivity as a function of density for various w/c ratios. The thermal conductivity of high strength lightweight raw perlite concrete increases with an increase in the density because of a decrease in the porosity inside the cement mortar and cement mortar occupation of raw PA porosities. The lowest thermal conductivity is obtained for the lowest water/cement ratio of 0.5. The thermal conductivity of concrete depends strictly on the thermal conductivities of the raw PA and cement binders. As is well known, the thermal conductivity of concrete can be decreased by the creation of air pores inside the concrete matrices for a constant amount of raw PA.

The effect of water absorption on the density is given in Fig. 5 for various water/cement ratios. Figure 5 shows that the water absorption percentage decreases as the specimen density increases while a similar trend was obtained from the plot of the thermal conductivity versus water absorption percentage as shown in Fig. 6.

It can be seen from Fig. 6 that the thermal conductivity of concrete decreases with an increase in the water absorption percentage. The lowest thermal conductivity is obtained for the highest water/cement ratio where $w/c = 0.65$. This trend may be due to the fact that the density of the cement is higher than that of other ingredients; thus, an increase in the cement amount results in an increase in density as reported by Uysal et al. [11]. It has also been seen that the thermal conductivity of concrete increases with increasing cement content.

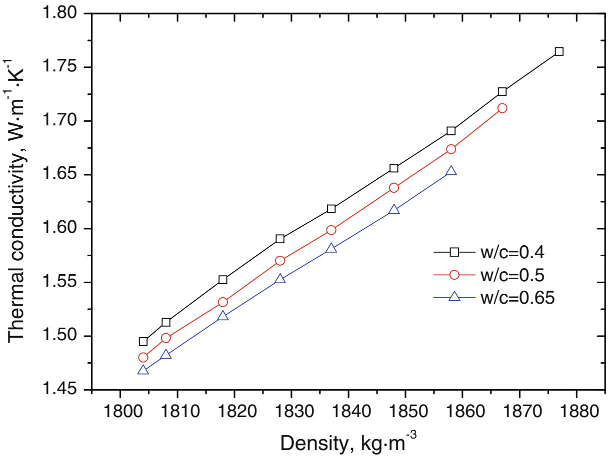

Fig. 4 Thermal conductivity versus density

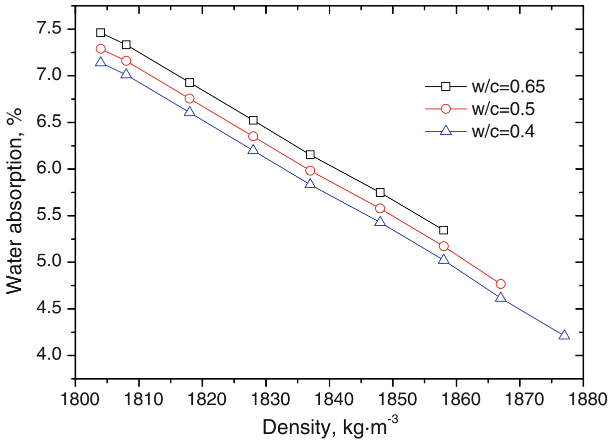

Fig. 5 Water absorption percentage versus density

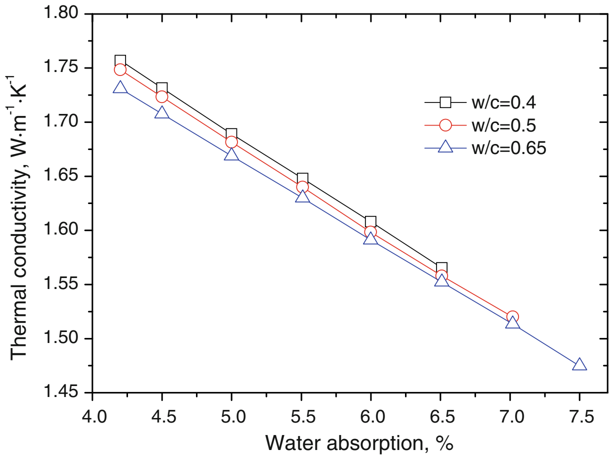

Fig. 6 Thermal conductivity versus water absorption percentage

In this study, a change in the water/cement ratio changes both the matrix structure of concrete and also the thermal conductivity of concrete. A decrease in the water/cement ratio inside the concrete decreases the air space ratio of concrete matrices and results in changes in the thermal conductivity. Figures 7, 8, and 9 show the effect of thermal conductivity on the mass ratio percentages of concrete constituents of water, perlite, and cement for $w/c = 0.4, 0.5$, and 0.65, respectively. It can be seen clearly from the figures that a decrease in the perlite mass ratio results in a decrease in the thermal conductivity. As the mass ratio of cement increases, so does the thermal conductivity. However, the results show that the thermal conductivity increases slightly with an increase in the water mass ratio for all water/cement ratios.

The thermal conductivity of HSLWPAC increases linearly with density as shown in Figs. 10, 11, and 12 at both room and low temperatures for water/cement ratios of

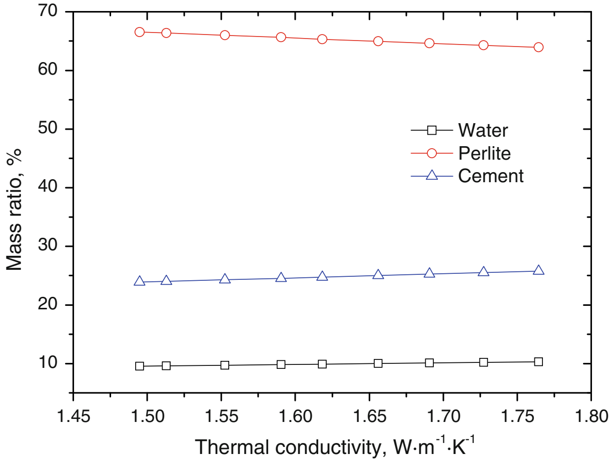

Fig. 7 The effect of thermal conductivity on mass ratio for $w/c = 0.4$

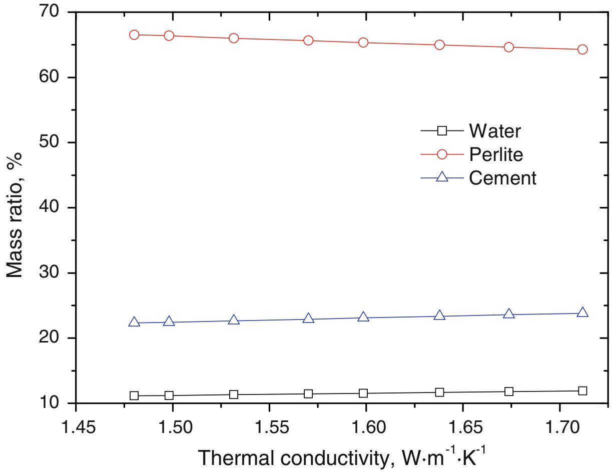

Fig. 8 The effect of thermal conductivity on mass ratio for $w/c = 0.5$

0.4, 0.5, and 0.65, respectively. The plots show that there is a significant reduction in the thermal conductivity at low temperatures as compared to room temperature independent of the water/cement ratio. As the density of concrete increases, the thermal conductivity of concrete increases for all water/cement ratios.

Figures 13, 14, and 15 show the thermal conductivities of HSLWPAC for water/cement ratios of 0.4, 0.5, and 0.65, respectively. Both the temperature and density of concrete have an obvious influence on the thermal conductivity, but the temperature is the main factor. Thus, a decrease in temperature has a positive effect on the thermal insulation capability by reducing the thermal conductivity. It can be seen that the maximum thermal conductivity of a designed concrete matrix is $1.777\ \mathrm{W \cdot m^{-1} \cdot K^{-1}}$ at 303.15 K for $w/c = 0.4$ which is about a factor of two larger than that of concrete.

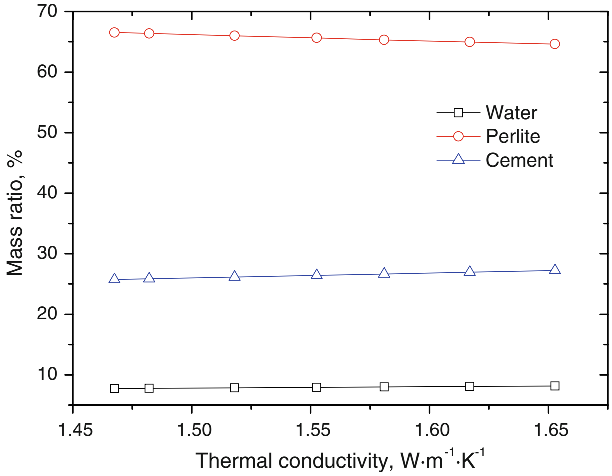

Fig. 9 The effect of thermal conductivity on mass ratio for $w/c = 0.65$

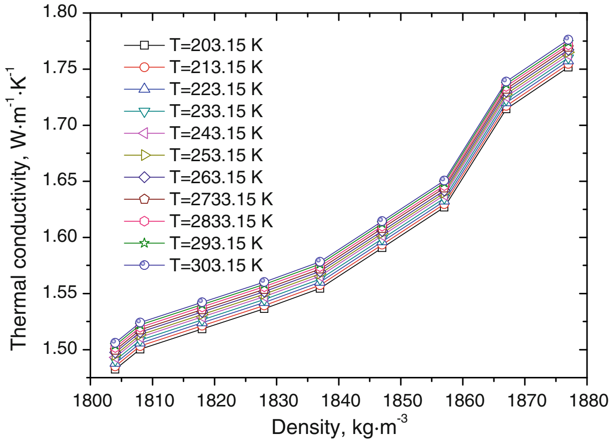

Fig. 10 Thermal conductivity charactericties for $w/c = 0.4$ at different temperatures

The largest thermal conductivity of concrete at room temperature reported in the literature [15] is in the range of $1.6\ \mathrm{W \cdot m^{-1} \cdot K^{-1}}$ to $3.6\ \mathrm{W \cdot m^{-1} \cdot K^{-1}}$.Therefore, the thermal conductivity of high strength lightweight concrete can be enhanced by using the Erzincan Mollaköy raw PA in concrete mixtures.

5 Conclusions

The present study has focused on the investigation of the thermal conductivity characteristics of HSLWPAC production from the Erzincan Mollaköy region. In mixed proportions of high strength lightweight concrete production, five different cement contents and eight different size diameters of raw PA were designed while keeping

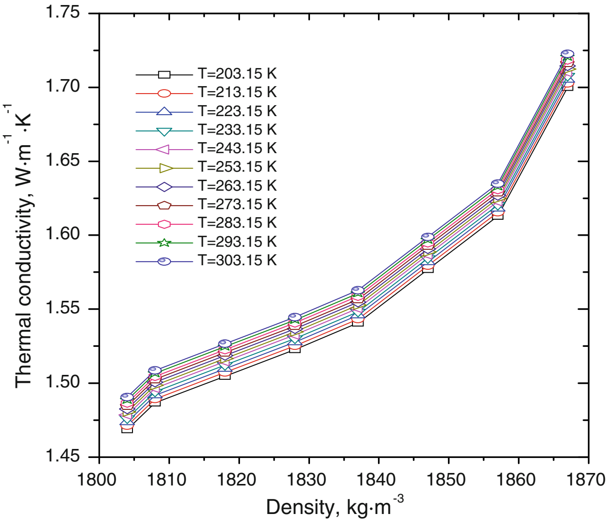

Fig. 11 Thermal conductivity characterictics for $w/c = 0.5$ at different temperatures

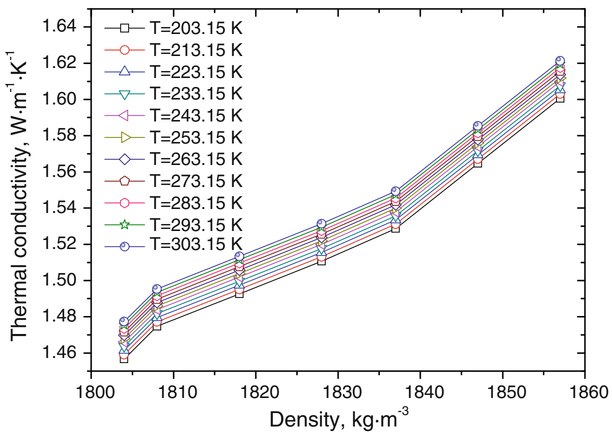

Fig. 12 Thermal conductivity characterictics for $w/c = 0.65$ at different temperatures

constant for three different w/c ratios of 0.4, 0.5, and 0.65 to assess and compare the thermal conductivity of high strength lightweight concrete by using raw PA from the Erzincan Mollaköy region in Turkey. In all cases, the amount of total raw PA for eight different diameters was kept constant and the content of water and cement was adjusted in order to obtain mixtures with the target w/c ratios and similar consistency. A comprehensive experimental study has been carried out by using two different thermal-conductivity measuring techniques within the range of temperature, $203.15\,\text{K} \leq T \leq 303.15\,\text{K}$. The thermal-conductivity measurement results are consistent for both measurement techniques, Almemo thermal conductivity sensor and QTM-500 quick thermal-conductivity meter. It was observed that the maximum

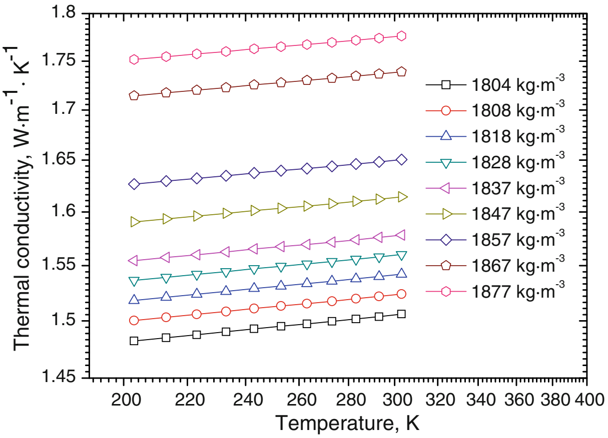

Fig. 13 Thermal conductivity characteristics for $w/c = 0.4$ at different densities

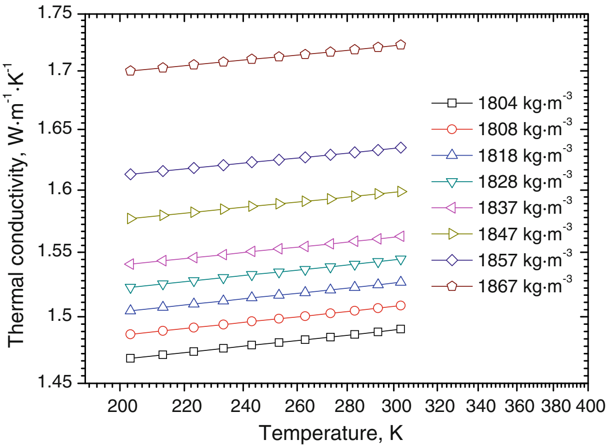

Fig. 14 Thermal conductivity characteristics for $w/c = 0.5$ at different densities

variation of thermal-conductivity values did not exceed 1.5 % for all types of concrete mixtures used in the test runs.

The effect of concrete matrix parameters on high strength lightweight concrete production can be explored by comparing the curves obtained from the experimental investigations. General empirical relations, which will be useful for estimation of concrete matrix optimizations, have been proposed for the thermal conductivity as functions of the water/cement ratio (w/c), raw perlite amount by mass (*PAP*), and temperature (T). The proposed empirical correlations of thermal conductivity, considered to be applicable within the range of temperatures $203.15\,\mathrm{K} \leq T \leq 303.15\,\mathrm{K}$, are in the form of

$$\lambda = a\left(PAP^{b}\right) + c\left(T^{d}\right)$$

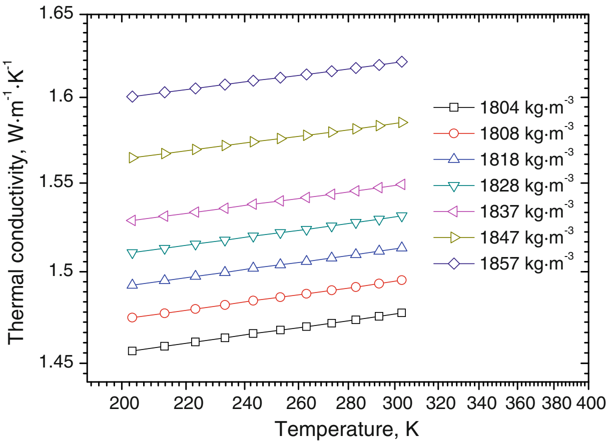

Fig. 15 Thermal conductivity characteristics for $w/c = 0.65$ at different densities

Table 4 Empirical correlations of thermal conductivity as a function of raw perlite aggregate percentage (*PAP*) and temperature (T) where $R^2 = 0.97927$

w/c	$\lambda = a\left(PAP^{b}\right) + c\left(T^{d}\right)$
0.4	$\lambda = 0.73376\left(PAP^{-0.24182}\right) + 299.92337\left(T^{0.99339}\right)$
0.5	$\lambda = 0.73057\left(PAP^{-0.23805}\right) + 304.50862\left(T^{0.98729}\right)$
0.65	$\lambda = 0.72374\left(PAP^{-0.21994}\right) + 311.06211\left(T^{1.04615}\right)$

Empirical correlations of derived thermal conductivity for designed HSLWPAC samples of three different water/cement ratios of 0.4, 0.5, and 0.65 are given in Table 4. The empirical correlation for thermal conductivities predicted 95 % of each set of experimentally observed thermal conductivity data within ±97.9 % accuracy over a range from $1.457\ \mathrm{W \cdot m^{-1} \cdot K^{-1}}$ to $1.777\ \mathrm{W \cdot m^{-1} \cdot K^{-1}}$. It can therefore be concluded that the proposed thermal conductivity correlations are reasonably satisfactory for the prediction of thermal conductivity for concrete matrices. The experimental investigation revealed that the usage of raw PA from the Erzincan Mollaköy region in concrete production reduces the concrete unit mass, increases the concrete strength, and furthermore, the thermal conductivity of the concrete has been improved. Based on experimental data and correlations for the thermal conductivity, the concrete matrices for the water/cement ratio of $w/c = 0.65$ at the lowest temperature where $T = 203.15\ \mathrm{K}$ should be preferred for the best performance because of the fact that it exhibits the lowest thermal conductivity number for high strength lightweight raw PA concrete production.

High strength lightweight raw PA concrete (HSLWPAC) from Erzincan Mollaköy region is a good thermal insulator at thermal conductivities from $1.457\ \mathrm{W \cdot m^{-1} \cdot K^{-1}}$ to $1.777\ \mathrm{W \cdot m^{-1} \cdot K^{-1}}$. More importantly, it has superior mechanical properties of compressive strength from 63 MPa to 80 MPa as compared with normal concrete at temperatures in the range, $203.15\ \mathrm{K} \leq T \leq 303.15\ \mathrm{K}$.

Acknowledgment The author gratefully acknowledges Mr. Düzgün Ürün of the Er-Per Company for valuable suggestions and donation of the Erzincan Mollaköy raw PAs used in this investigation.

References

1. E. Yasar, C.D. Atis, A. Kilic, H. Gulsen, Mater. Lett. **57**, 2267 (2003)
2. M.A. Riley, Mag. Concr. Res. **43**, 87 (1991)
3. T.A. Hammer, *Compressive Strength and e-Modulus of Elevated Temperatures*. Trondheim: Report 6.1, High Strength Phase 3.SIN- TEF-Report No. STF70 A 95023 (1995)
4. M. Saad, S.A. Abo-El-Enein, G.B. Hanna, M.F. Kotkata, Cem. Concr. Compos. **26**, 669 (1996)
5. E. Sancak, Y.D. Sari, O. Simsek, Cem. Concr. Compos. **3**, 715 (2008)
6. Y. Xu, D.D.L. Chung, Cem. Concr. Res. **30**, 1305 (2000)
7. R. Gul, H. Uysal, R. Demirboga, Kocapınar Pomzası ile Üretilen Hafif Betonların Isı İletkenliklerinin Araştırılması (Investigation of the thermal conductivity of lightweight concrete made with Kocapınar's pumice aggregate), Advances in Civil Engineering: III. Technical Congress, vol. 2 (METU, Ankara, Turkey, 1997), pp. 553–562 [in Turkish]
8. T. Ashworth, E. Ashworth, in *Insulation Materials: Testing and Applications*, ed. by R.Ş. Graves, D.C. Wysocki, ASTM Special Tech. Pub., vol. 1116 (ASTM, West Conshohocken, PA, 1991), pp. 415–429
9. FIP State of Art Report, *Principles of Thermal Insulation with Respect to Lightweight Concrete*, FIP/8/1, C and CA (Slought, England, 1978)
10. A. Bouguerra, A. Ledhem, F. de Barquin, R.M. Dheilly, M. Queneu-dec, Cem. Concr. Res. **28**, 1179 (1998)
11. H. Uysal, R. Demirboğa, R. Şahin, R. Gül, Cem. Concr. Res. **3**, 845 (2004)
12. R. Demirboğa, Build. Environ. **42**, 2467 (2007)
13. R. Demirboğa, I. Türkmen, M.B. Karakoç, Build. Environ. **42**, 349 (2007)
14. H. Çanakci, R. Demirboğa, M.B. Karakoç, O. Şirin, Build. Environ. **42**, 1777 (2007)
15. A.M. Neville, *Properties of Concrete* (Longman, UK, 1995)
16. A.M. Neville, *Properties of Concrete* (Właściwości Betonu), (Polski Cement, Cracow, 2000) [in Polish]
17. I.B. Topcu, Cem. Concr. Res. **27**, 15 (1997)
18. H. Al-Khaiat, M.N. Haque, Cem. Concr. Res. **28**, 859 (1998)
19. A. Kılıç, C.D. Atiş, E. Yaşar, F. Özcan, Cem. Concr. Res. **33**, 1595 (2003)
20. İ. Ulusu, Ham perlit agregası kullanarak yüksek dayanımlı hafif beton üretilebilirliğinin araştırılması, Ph.D. Thesis (Fen Bilimleri Enstitüsü, Atatürk Üniversitesi, Doktora tezi, 2007) [in Turkish]
21. Ç. Meral, *Use of Perlite as a Pozzolanic Addition in Blended Cement Production* (M.S. Thesis, The Graduate School of Natural and Applied Sciences, Middle East Technical University, 2004)
22. ASTM C 311-02, *Standard Test Methods for Sampling and Testing Fly Ash or Natural Pozzolans for use as a Mineral Admixture in Portland-Cement Concrete*, Annual Book of ASTM Standards, vol. 04.02 (2002)
23. Erzincan Mollaköy Perlite Investigation Reports Information. Web Page of Er-Per Company, http://www.er-per.com/rapor.php
24. ASTM C39, *Standard Test Method for Compressive Strength of Lightweight Insulating Concrete*, Annual Book of ASTM Standards (2002)
25. ASTM C567-05a, *Standard Test Method for Determining Density of Structural Lightweight Concrete*, Annual Book of ASTM Standards (2005)
26. A. Franco, Appl. Therm. Eng. **27**, 2495 (2007)
27. ASTM C 1113-90, *Test Method for Thermal Conductivity of Refractories by Hot Wire (Platinum Resistance Thermometer Technique)*, Annual Book of ASTM Standards (1990)
28. W.R. Daire, A. Downs, Trans. Br. Ceram. Soc. **79**, 44 (1980)
29. J.C. Willshee, in *Proceedings of British Ceramic Society* **29**, 153 (1980)
30. K. Sengupta, R. Das, G. Banerjee, J. Test. Eval. **29**, 455 (1992)